Advanced materials based on azulenyl-phenyloxazolone

Alina-Giorgiana Brotea, Ovidiu-Teodor Matica, Cornelia Musina (Borsaru), Mihaela Cristea, Amalia Stefaniu, Andreea Madalina Pandele, Eleonora-Mihaela Ungureanu

Basic properties for **M** and characterization by elemental analysis, UV-Vis, ^{1}H NMR, ^{13}C-NMR, IR, MS

2-Phenyl-4-((4,6,8-trimethylazulen-1-yl)methylene)oxazol-5(4H)-one, (M). Dark violet crystals, m.p. 214–216 °C. UV-Vis (MeOH), λ(log ε): 243 (4.43), 295 sh (3.97), 329 (4.14), 404 sh (3.92), 486 (4.40). ^{1}H-NMR (300 MHz, $CDCl_3$, 20 °C): 2.63 (s, 3 H, Me), 2.89 (s, 3 H, Me), 3.19 (s, 3 H, Me), 7.25 (s, 1 H, 5-H), 7.26 (s, 1 H, 7-H), 7.46 (d, ^{3}J = 4.7 Hz, 1 H, 3-H), 8.17 (dd, ^{3}J = 7.9 Hz, ^{4}J = 1.5 Hz, 2 H, 2′-H, 6-H), 7.48–7.55 (m, 3 H, 3′-H, 4′-H, 5′-H), 8.25 (s, 1 H, CH=), 9.16 (d, ^{3}J = 4.7 Hz, 1 H, 2-H) ppm. ^{13}C-NMR (75.47, MHz, $CDCl_3$, 20 °C): 26.0, 28.4, 30.1, 119.8, 125.6, 126.6, 127.7, 128.8, 129.1, 129.5, 132.0, 132.1, 133.8, 138.1, 139.9, 142.6, 146.9, 148.1, 148.2, 160.3, 169.0 ppm. IR (neat): 3103 w, 2918 vs, 2855 s, 2175 w, 1723 vs, 1612 s, 1571 s, 1490 s, 1517 s, 1403 s, 1318 s, 1265 vs, 1152 s, 1020 s, 839 m, 698 m cm^{-1}. MS (+ESI): 342 [M+1]. Calcd. for $C_{23}H_{19}NO_2$: C, 80.92; H, 5.61; N, 4.10. Found: C, 80.90; H, 5.60; N, 4.13.

Table S1. Potentials *vs.* Fc/Fc^{+} (Epa, Epc) and currents (ipa, ipc) of Fc anodic and cathodic peaks in 3 mM Fc solution in 0.1 M TBAP/ CH_3CN for GC bare electrode and for the **M**-CMEs prepared by scanning in solution with [**M**] = 2 mM in 15 successive cycles on different anodic potential domains.

Crt. Nr.	Electrode (domain of scanning in V)*1	Epa (V)	$10^5 \cdot$ ipa (A)	Epc (V)	$10^5 \cdot$ ipc (A)	ΔEp *2 (mV)	Ef *3 (V)
1	GC bare electrode	0.052	8.838	–0.049	-–5.390	101	0.050
2	CME 1 (0 - 0.6)	0.064	5.223	–0.043	–3.215	107	0.054
3	CME 2 (0 – 0.8)	0.054	5.170	–0.048	–3.209	102	0.051
4	CME 3 (0 - 1.2)	0.056	5.187	–0.048	–3.127	104	0.052
5	CME 4 (0 - 1.4)	0.053	5.187	–0.047	–3.110	100	0.050

*1Anodic potential domains of scanning (*vs.* RE) during **M**-CME preparation; *2 ΔEp = Epa – Epc; *3 Ef = (Epa + Epc)/ 2

Table S2. Main characteristics of the DPV peaks recorded on **M**-CMEs (obtained by CPE at 0.6 V and 1 mC) for different concentrations of mixed metals in the aqueous accumulation solution.

Crt. Nr.	[HM], M	E Cd (V)	E Pb (V)	E Cu (V)	E Hg (V)	$10^8 \cdot$i Cd (A)	$10^8 \cdot$i Pb (A)	$10^8 \cdot$i Cu (A)	$10^8 \cdot$i Hg (A)
1	10^{-4}	-	–0.52	–0.06	0.27	-	2270	66	117
2	$5 \cdot 10^{-5}$	-	–0.51	–0.07	0.22	-	1590	39.3	137
3	10^{-5}	-	–0.52	–0.10	0.20	-	885	7.8	51.4
4	$5 \cdot 10^{-6}$	– 0.80	–0.54	-	0.16	4.1	298	-	1.1
5	10^{-6}	-	–0.54	-	-	-	480	-	-
6	$5 \cdot 10^{-7}$	-	–0.56	-	-	-	156	-	-
7	10^{-7}	-	–0.57	-	-	-	184	-	-
8	$5 \cdot 10^{-8}$	-	–0.57	-	-	-	148	-	-
9	10^{-8}	-	–0.57	-	-	-	128	-	-
10	$5 \cdot 10^{-9}$	-	–0.57	-	-	-	84	-	-
11	10^{-9}	-	–0.58	-	-	-	6.3	-	-
12	$5 \cdot 10^{-10}$	-	–0.59	-	-	-	2.4	-	-

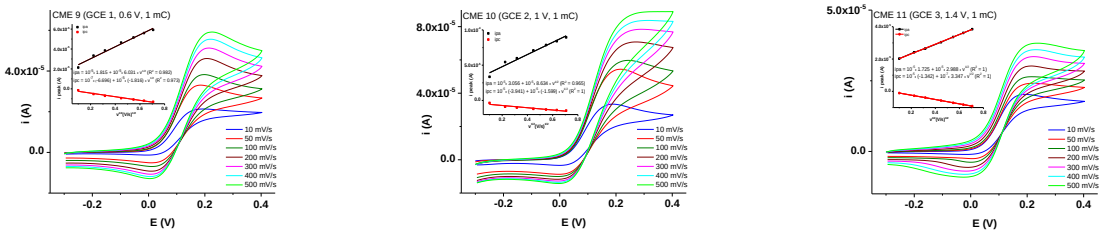

(a) (b) (c)

Figure S1. Study of the scan rate influence on Fc Cv curves recorded on **M**-CMEs prepared on: GCE 1 (CME 9, 0.6 V, 1 mC) (a); GCE 2 (CME 10, 1 V, 1 mC) (b) ; GCE 3 (CME 11, 1.4 V, 1 mC). Insets: linear dependences of the peak currents (ipa and ipc) on the square root of the scan rate, for each electrode with slope of: $6.031 \cdot 10^{-5}$ A·(V/s)$^{-1/2}$ (CME 9); $8.634 \cdot 10^{-5}$ A·(V/s)$^{-1/2}$ (CME 10); $2.988 \cdot 10^{-5}$ A·(V/s)$^{-1/2}$ (CME 11).

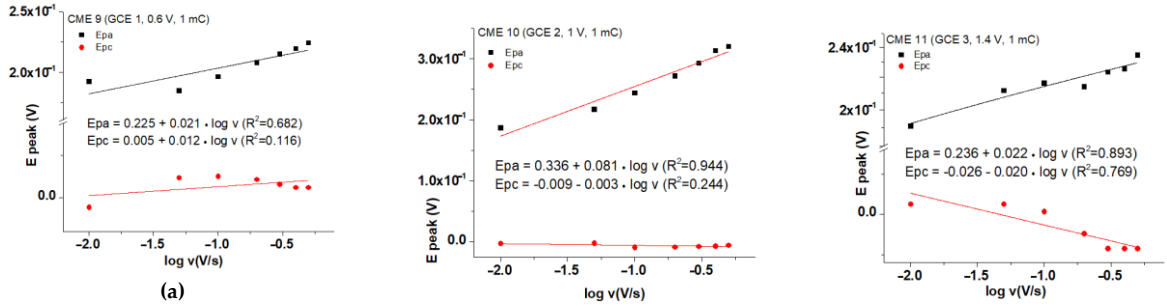

(a) (b) (c)

Figure S2. Variation of the peak potential of Fc in 5 mM solution in 0.1 M TBAP/ CH_3CN (Epa) *vs* log v (v in V/s for: CME 9 (a), CME 10 (b), CME 11 (c) with slopes of: 0.021 V (CME 9); 0.081 V (CME 10); 0.022 V (CME 11), respectively, for Epa and of 0.012 V (CME 9); 0.003 V (CME 10); 0.020 V (CME 11), respectively, for Epc.

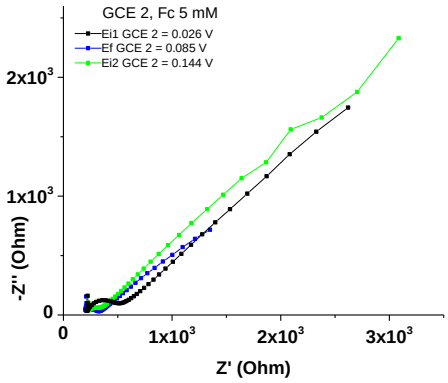

Figure S3. Impedance curves in Fc 5 mM for the bare electrode GCE 2 (1 V, 1 mC) at equilibrium potential Eeq = 0.085 V (blue), and at imposed potentials Ei1 = 0.026 V (black), and Ei2 = 0.144 V (green), respectively.

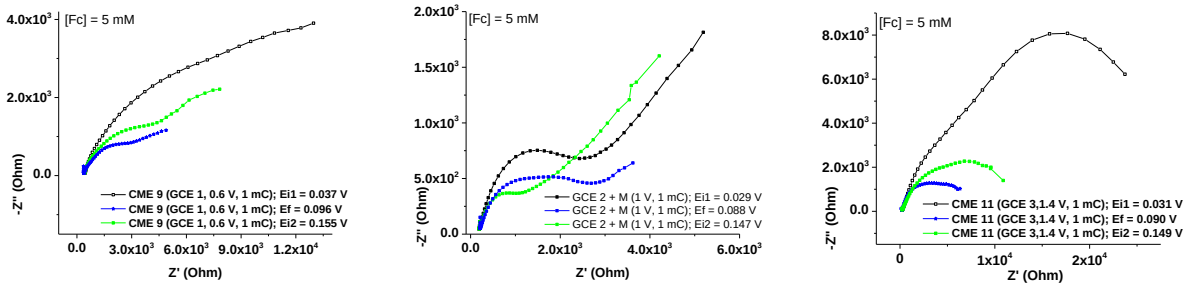

(a) (b) (c)

Figure S4. Impedance curves recorded in Fc 5 mM at different potentials on : CME 9 (obtained at 0.6 V) at Ei1 = 0.037 V (black), Eeq = 0.096 V (blue), Ei2 = 0.155 V (green); CME 10 (obtained at 1 V) at Ei1 = 0.029 V (black), Eeq = 0.088 V (blue), Ei2 = 0.147 V (green); CME 11 (obtained at 1.4 V) at Ei1 = 0.031 V (black), Eeq = 0.090 V (blue), Ei2 = 0.149 V (green).

(a)

(b)

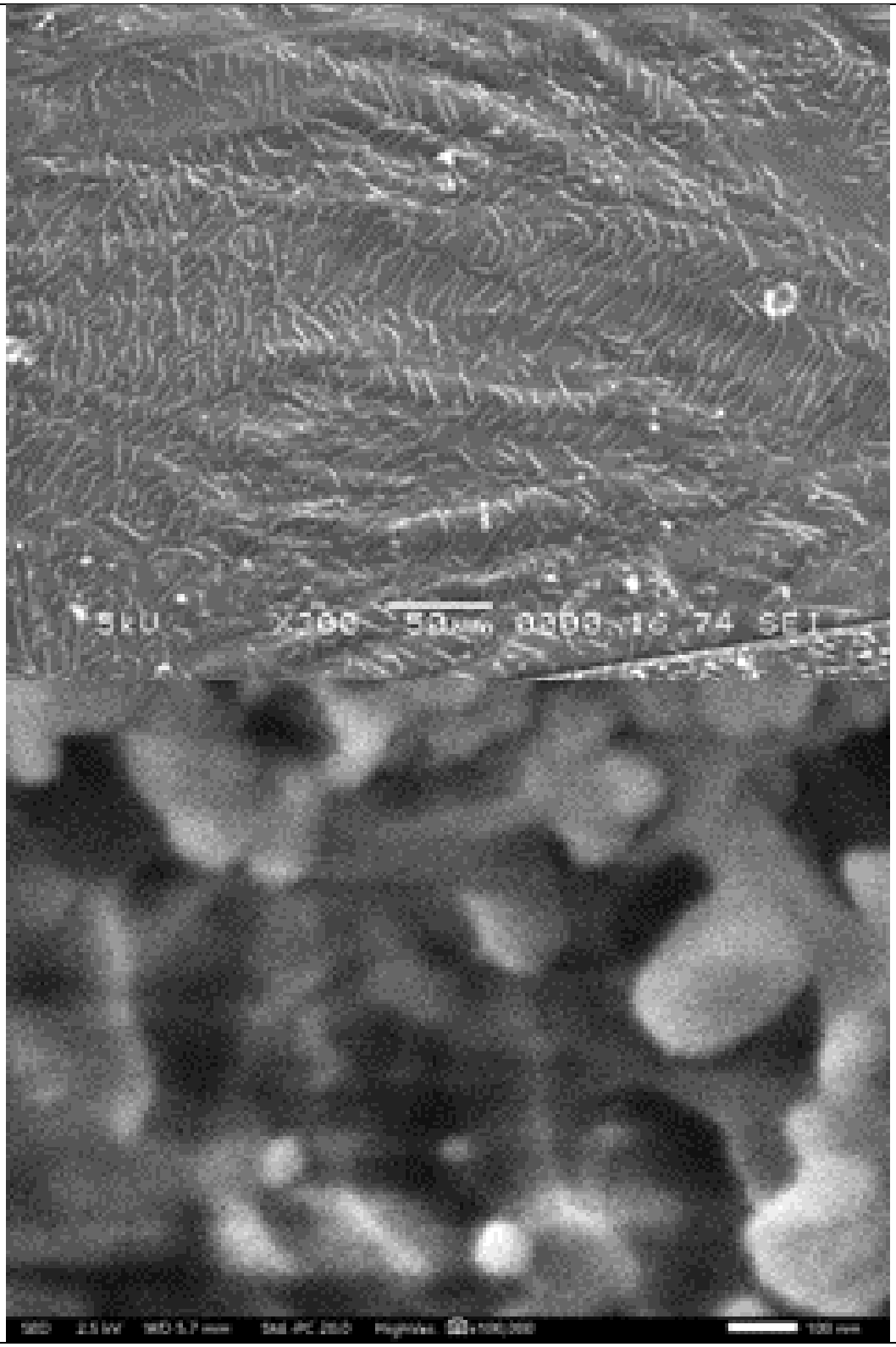

Figure S5. SEM images of the polymer surfaces obtained by CPE at 1.4 V, 4 mC (14 mC/cm^2) (CME 12) at two magnifications: x300, 5 kV (a) and x10^5, 2.5 kV (b).

(a)

(b)

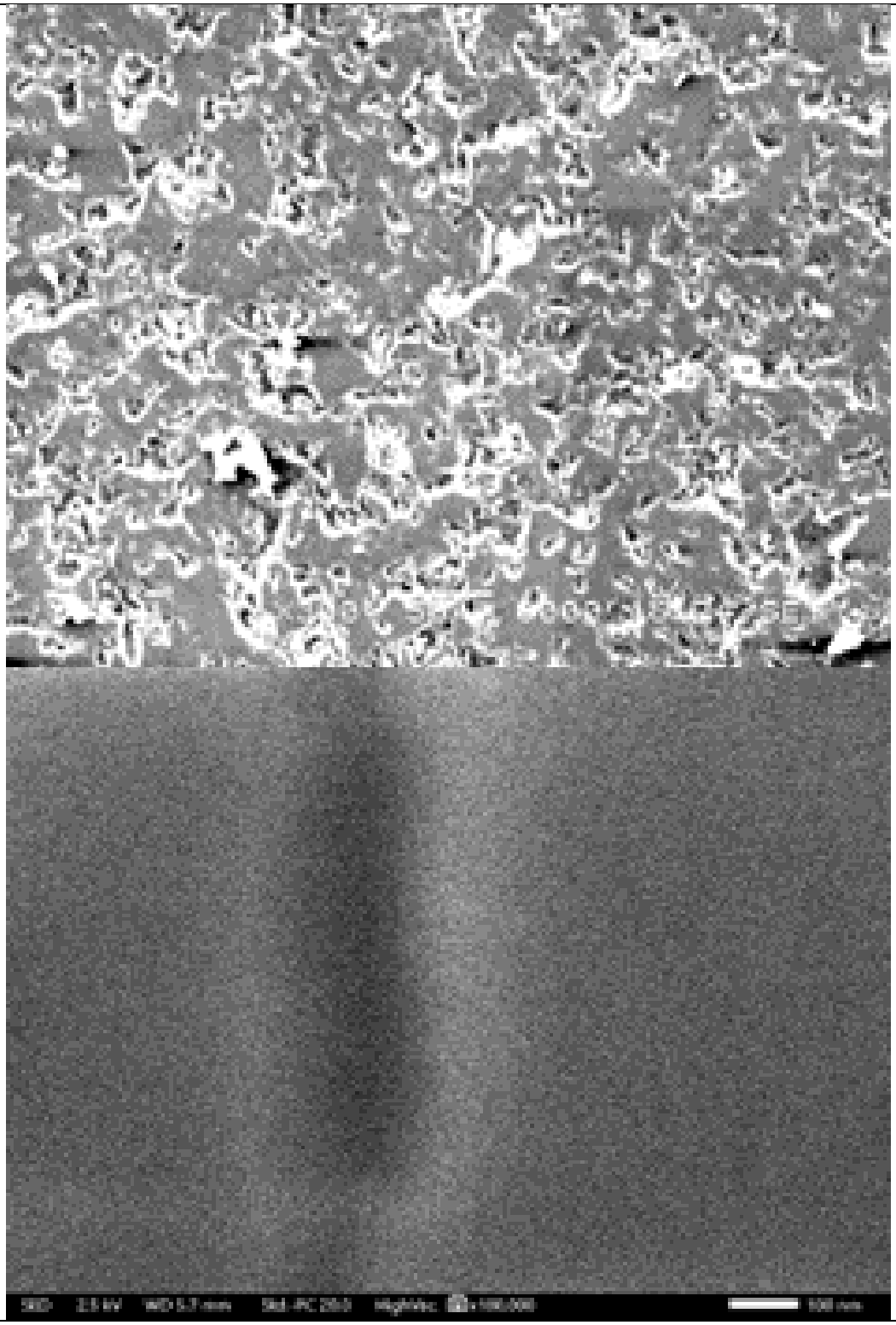

Figure S6. SEM images of the polymer surfaces obtained by CPE at 1 V, 4 mC (14 mC/cm^2) (CME 13) at two magnifications: x300, 5 kV (a) and x10^5, 2.5 kV (b).

(a)

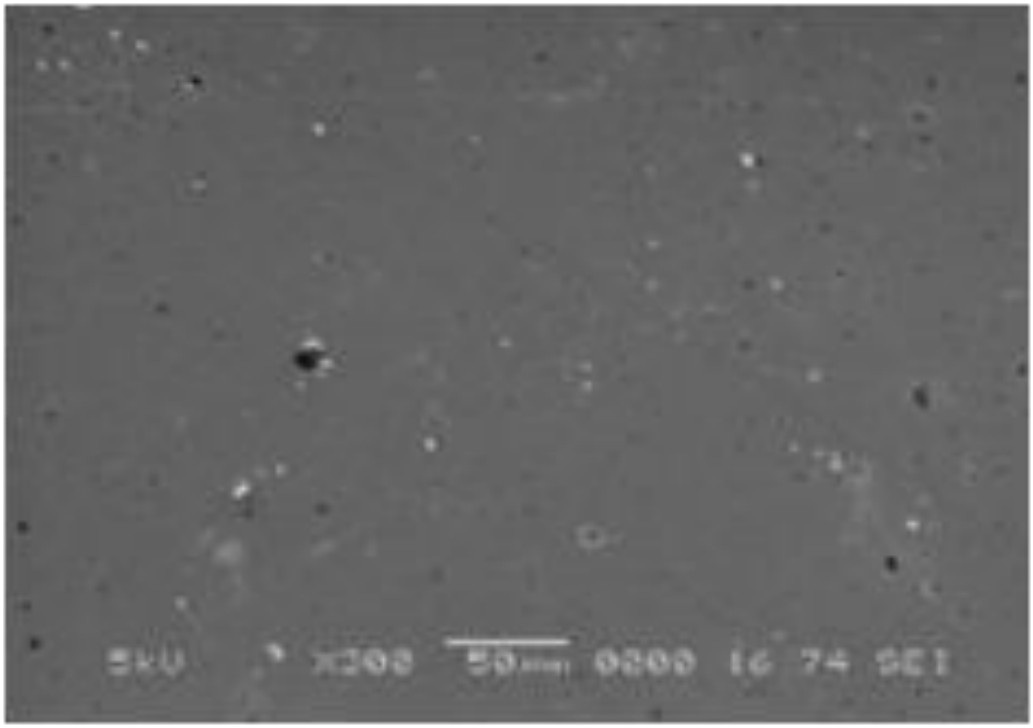

(b)

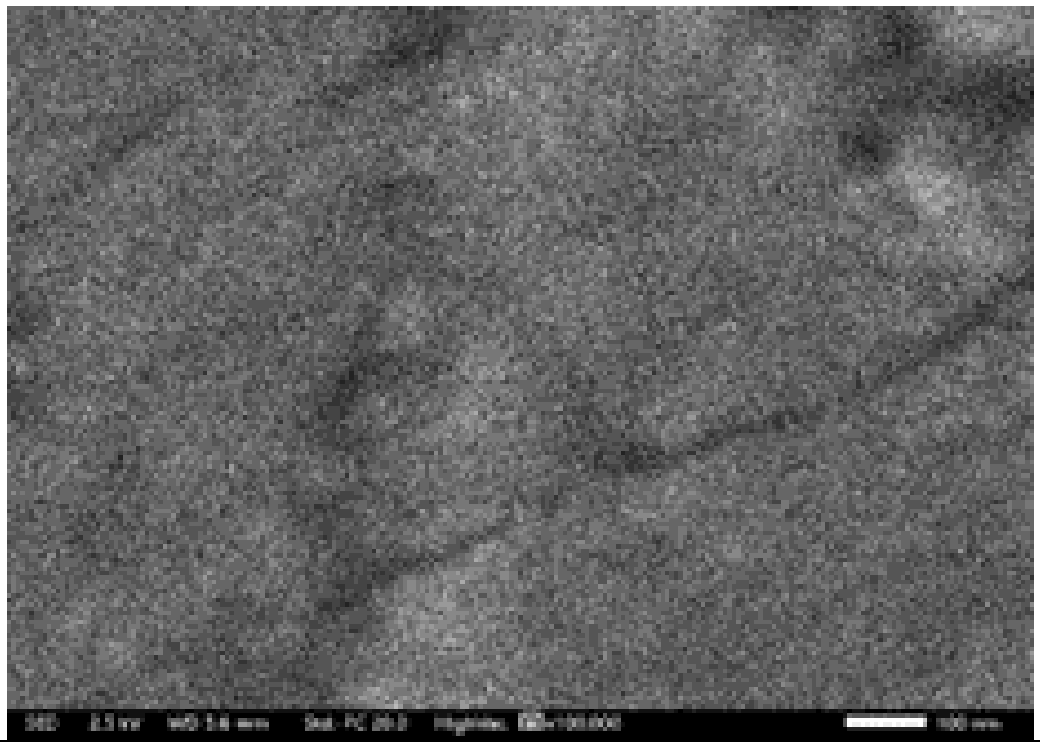

Figure S7. SEM images of the polymer surfaces obtained by CPE at 0.6 V, 4 mC (14 mC/cm^2) (CME 14) at two magnifications: x300, 5 kV (a) and x10^5, 2.5 kV (b).

(a)

(b)

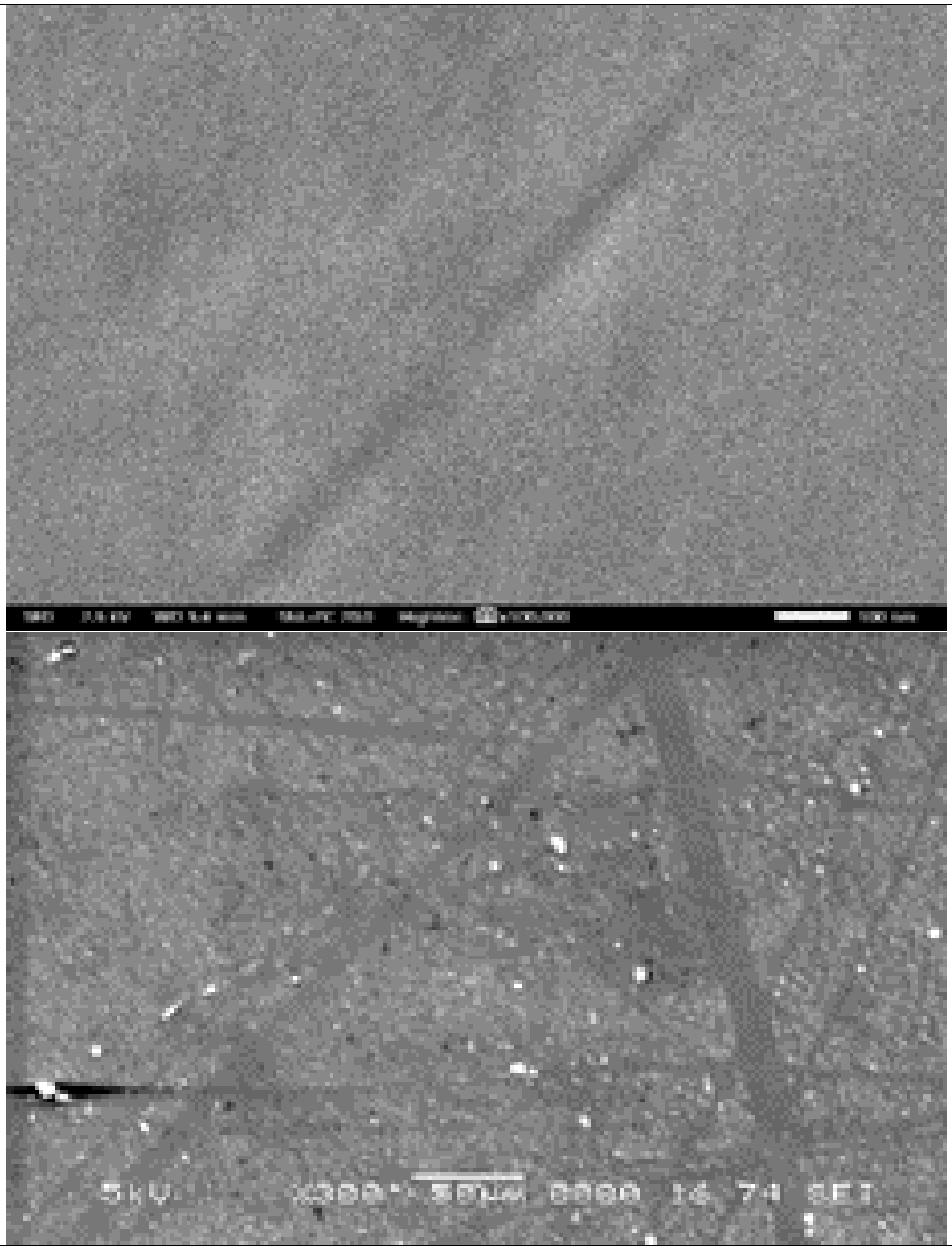

Figure S8. SEM images of the polymer surfaces obtained by CPE at 0.6 V, 8 mC (28 mC/cm^2) (CME 15) at two magnifications: x300, 5 kV (a) and x10^5, 2.5 kV (b).

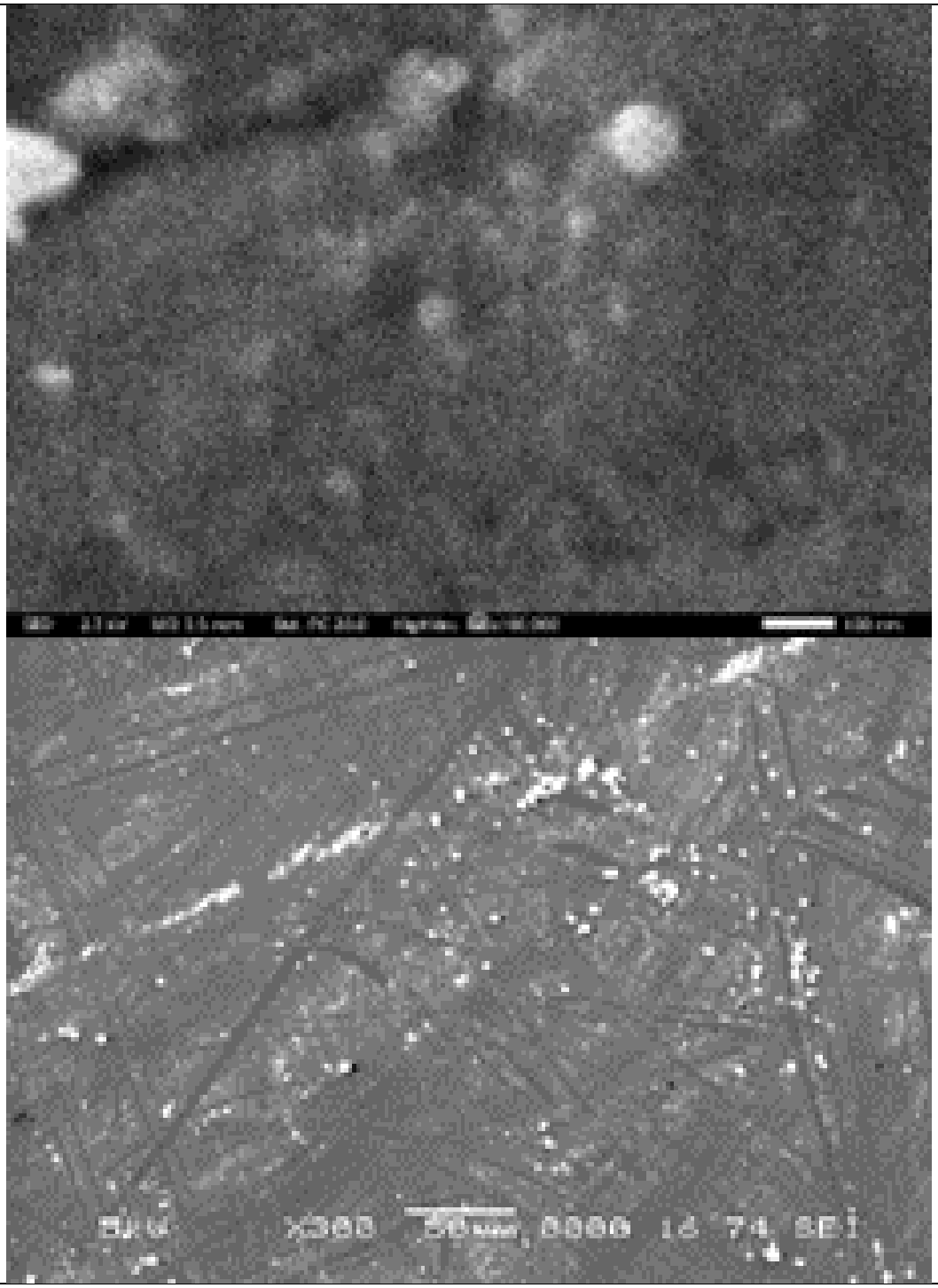

Figure S9. SEM images of the polymer surfaces obtained by CPE at 0.6 V, 16 mC (56 mC/cm^2) (CME 16) at two magnifications: x300, 5 kV (a) and x10^5, 2.5 kV (b).

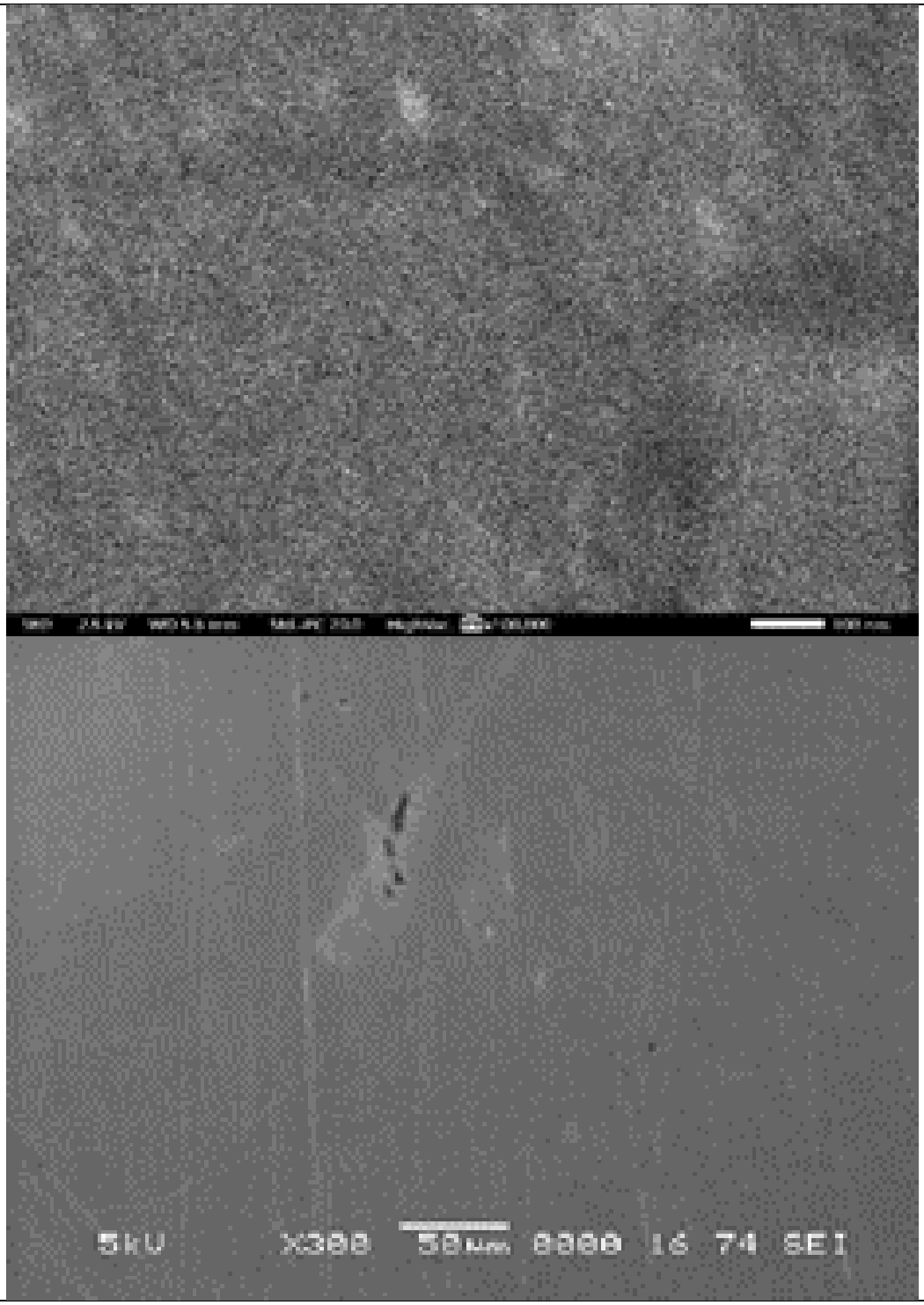

Figure S10. SEM images of the polymer surfaces obtained by CPE at 0.6 V, 24 mC (84 mC/cm^2) (CME 17) at two magnifications: x300, 5 kV (a) and x10^5, 2.5 kV (b).

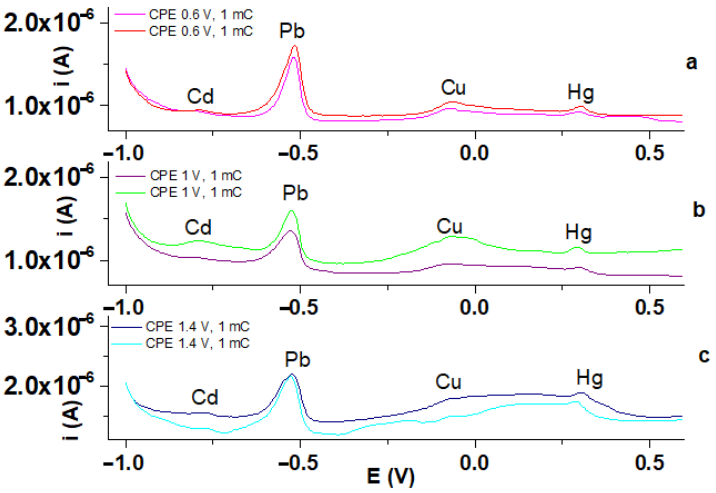

Figure S11. DPV curves (0.01 V s-1) recorded on **M**-CMEs, prepared by CPE at 1 mC and different potentials: 0.6 V (a), 1 V (b), and 1.4 V (c), corresponding to $5 \cdot 10^{-6}$ M concentration of each mixed metal ions.